

Toward Quantitative Prediction of Stereospecificity of Metallocene-Based Catalysts for α -Olefin Polymerization

Klaus Angermund,* Gerhard Fink,* Vidar R. Jensen, and Ralph Kleinschmidt

Max-Planck Institut für Kohlenforschung, D-45470 Mülheim an der Ruhr, Germany

Received October 19, 1999

Contents

I. Introduction	1457
II. π Complex Model	1457
III. Combined QM/MM Approaches	1459
IV. From Energy Differences to Pentad Distributions	1464
V. Systematic and Independent Prediction of Pentad Distributions	1465
VI. Further Treatment of Temperature Effects	1467
VII. Present State and Outlook	1468
VIII. Acknowledgment	1469
IX. References	1469

I. Introduction

Chiral metallocene-based catalysts for α -olefin polymerization¹ are characterized by a well-defined active center², forming a sound basis for establishing relationships between the molecular structure of the catalyst and the microstructure of the resulting polymer. The importance of the local structure and symmetry of the active center was understood already for the classical Ziegler–Natta catalysts, but conclusive evidence regarding the relationship was difficult to achieve due to lack of structural information about the active center. However, already in 1971, Allegra³ concluded that the active center in TiCl_3 -based catalysts for isospecific α -olefin polymerization must possess local C_2 symmetry since the regular, intermediate-chain migration (back-skip) required by the Cossée and Arlman^{4–6} mechanism should have a higher barrier than that of a new insertion. Today, simple symmetry-based rules for the relationship⁷ between the structure of the active metallocene cation and the tacticity of the polymer are well-known and useful for gaining insight into the mechanism of polymerization as well as practical tools for developing new catalysts. At the same time, it is evident that a complete description of the subtle nature of this relationship requires more than qualitative symmetry rules, and computational efforts, to be described below, have been undertaken to refine the picture. Because a review covering the whole research field of computational investigation of transition metal catalyzed alkene polymerization will be presented by Rappé et al.⁸ elsewhere in this edition of *Chemical Reviews*, we will limit our account to encompassing contributions closely related to modeling of stereospecificity for metallocene-based α -olefin

polymerization in the homogeneous phase, a field dating back to the late 1980s. Particular focus is put on recent, in part unpublished, efforts based on schemes combining quantum mechanics (QM) and molecular mechanics (MM), which attempt a more accurate prediction of the polymer microstructure.

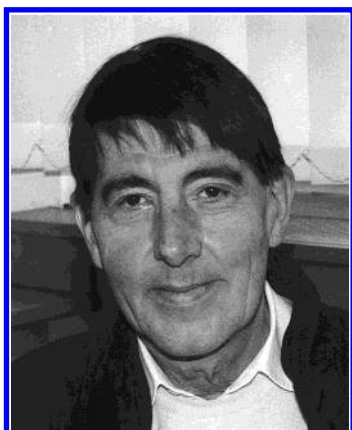
II. π Complex Model

The first force-field-based investigation of stereocontrol in homogeneous metallocene-catalyzed 1-alkene polymerization, published by Corradini and co-workers in 1988,⁹ focused on the isospecific propene polymerization using the C_2 -symmetric *rac*-ethylenebis(4,5,6,7-tetrahydroindenyl)titanium dichloride catalyst. This work was based in part on the authors' contributions to the field of heterogeneous Ziegler–Natta polymerization, with publications dating back to 1979.^{10–15} Turning to polymerization in the homogeneous phase, Corradini and co-workers⁹ used the crystal structure of the catalyst precursor (the dichloride) and replaced the chlorine atoms by the first carbon atom of the growing polymer chain and the center of the double bond of the coordinated propene, respectively. Values for missing bond lengths and valence angles were set to typical values as found in crystal structures. Of particular importance are the structural parameters pertaining to the coordination of the olefin because of the unstable nature of d^0 metal–alkene complexes. The necessary parameters were thus taken from the crystal structure of a d^2 metal–ethylene complex, bis(pentamethylcyclopentadienyl) titanium(II).¹⁶ The thus obtained preinsertion complex (π complex) of propene with ethyl as model of the growing polymer chain is shown in Figure 1.

With the exception of two valence angles (α and β) and two torsion angles (ϑ_0 and ϑ_1) (cf. Figure 2), the structure was kept fixed during all calculations. Applying a molecular mechanics scheme mainly based on nonbonded interactions, they determined the energy profiles for the rotations ϑ_0 and ϑ_1 . They found that structures where the second carbon atom of the chain avoids having close (repulsive) contact with the ligand ($\vartheta_1 \approx -50^\circ$), as shown in Figure 2, are highly preferred. It should be noted that the second carbon atom was not allowed to relax to positions on the opposite side ($\vartheta_1 \approx 180^\circ$) with respect to the olefin as this would violate the principle of “least nuclear motion”.^{17–19}



Klaus Angermund, born 1958, studied chemistry at the Heinrich-Heine-University of Düsseldorf, Germany. From 1983 to 1986, he worked as a Ph.D. student under the supervision of Carl Krüger in the X-ray department at the Max-Planck-Institut für Kohlenforschung in Mülheim an der Ruhr (Germany). In 1986, he obtained his Ph.D. in Chemistry from the University of Wuppertal (Germany) with a thesis about high-resolution X-ray crystallography. In 1987, he was awarded an Otto-Hahn scholarship by the Max-Planck society and worked from 1987 to 1988 as a postdoctoral fellow with Arnold Hagler at Biosym Techn. Inc. in San Diego. Since 1989, he has been a scientific coworker at the Max-Planck-Institut für Kohlenforschung and head of the molecular modeling group. In 1997, he was appointed an academic lecturer for crystallography and molecular modeling at the Ruhr-University of Bochum (Germany). Areas of research: application of molecular modeling techniques to organometallic reaction, force field development, and parameterization.



Gerhard Fink, born 1939, obtained his Doctor in Chemistry degree (Dr. rer. nat.) from the Technical University of München in 1969 with a biophysical thesis under the direction of Franz Patat. In 1977, he became recognized as academic lecturer (Habilitation) for Chemistry from the same university with a work on elementary steps in Ziegler-Natta-Catalysis. Since 1980, he has been the head of the macromolecular research group at the Max-Planck-Institut für Kohlenforschung in Mülheim an der Ruhr, Germany. He is apl. Professor and lecturer for macromolecular chemistry at the University of Düsseldorf. Areas of research: kinetics, mechanisms, and elementary processes; homogeneous and heterogeneous polymerization catalysis, including reaction modeling; and stereospecific polymerization and polymer reaction engineering.

Considering only structures where the latter is pointing away from the ligand, as in both panels A and B in Figure 1, the alternative (A) where the methyl group of propene and the second carbon atom are on opposite sides of the plane defined by the metal and the double bond of propene (given $\vartheta_0 \approx 0^\circ$) was, as expected, found to be the most stable. In the case of a (R,R) coordinated [as opposed to (S,S)] chelating ligand,^{20,21} the preferred coordination face of the prochiral propene is termed *re* according to



Vidar R. Jensen was born in 1966 in Kristiansand, Norway, and obtained his Ph.D. in Chemistry from the Norwegian Institute of Technology in 1995, with a thesis on the mechanism of Ziegler-Natta catalyzed polymerization under the direction of Martin Ystenes. He was a VISTA postdoctoral fellow (1995–1996) in the group of Knut J. Børve at the University of Bergen, Norway, and a NFR (Norwegian Research Council) postdoctoral fellow (1997–1998) at the Max-Planck Institut für Kohlenforschung, Germany, where he is currently working in the theory group of Walter Thiel. His research interest is organometallic chemistry with a particular focus on the application of computational methods to the investigation of mechanisms of transition metal catalyzed reactions as well as to the design of new organometallic catalysts.



Ralph Kleinschmidt was born 1970 in Krefeld, Germany. He studied chemistry at the University of Düsseldorf (Germany). From 1996 to 1999, he worked as a Ph.D. student at the Max-Planck-Institut für Kohlenforschung in Mülheim an der Ruhr (Germany) in the group of Gerhard Fink. In 1999, he obtained his Ph.D. in chemistry from the University of Düsseldorf with a thesis about the synthesis of metallocene and half-sandwich metallocene complexes and their application as catalysts in the α -olefin homo- and co-polymerization.

rules given by Hanson.²² The first three contributions from Corradini and Guerra et al.^{9,23,24} concerning homogeneous, isospecific polymerization were soon extended to covering the formation of syndiotactic polypropene.²⁵ For C_s or C_1 symmetric catalysts, the metal atom itself is a stereogenic center with two different coordination sites, leading to the formation of (R) and (S) complexes.^{20,21} Each of the latter may have either a *re* or a *si* coordinated propene, giving rise to the four diastereomeric metal-propene complexes *Rre*, *Rsi*, *Sre*, and *Ssi*. Guerra et al.²⁵ again noted the indirect influence of the catalyst ligand upon the coordination face of the propene: the chiral catalyst complex imposes a distinct orientation of the chain, which in turn strongly favors a coordination of propene minimizing the repulsion between

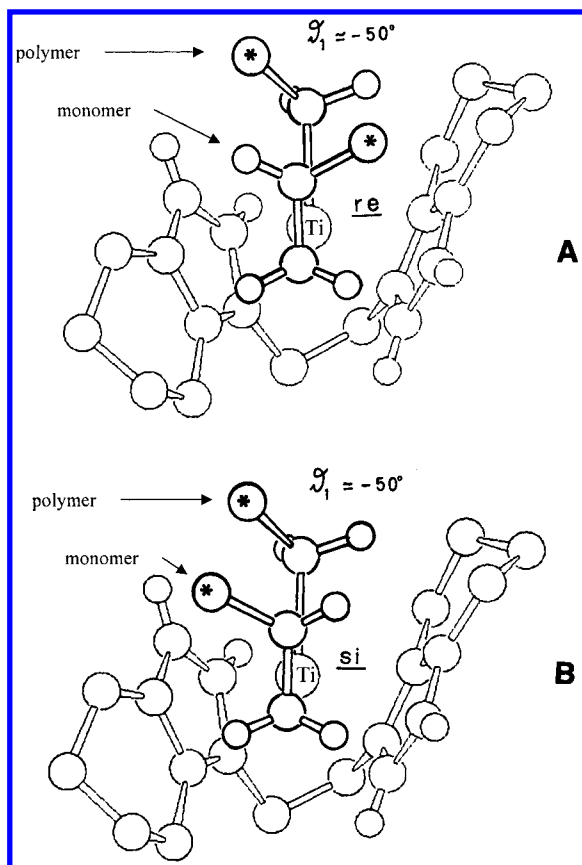


Figure 1. Preinsertion complex (π complex) of propene with ethyl as model of the growing polymer chain for the ethylenebis(1-indenyl) ligand. (*) Methyl groups. (A) *re*-facial coordination of propene with anti conformation of the two methyl groups; (B) *si*-facial coordination of propene with syn conformation of the two methyl groups. For definition of ϑ_1 , see Figure 2.¹⁰⁴ (Reprinted with permission from ref 9. Copyright 1988.)

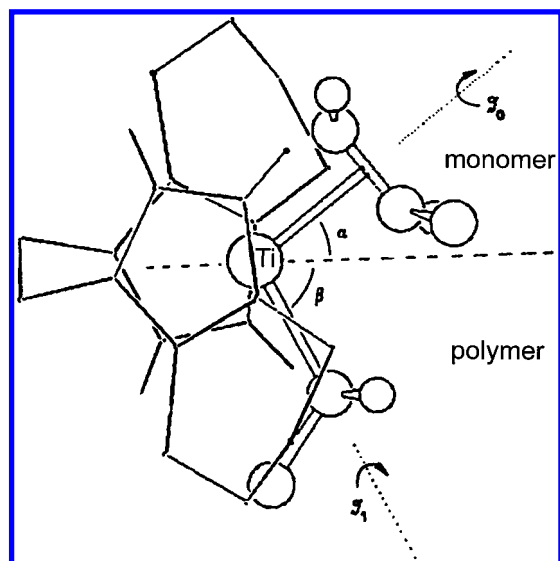


Figure 2. The catalytic model (Figure 1) showing the local C_2 symmetry axis.¹⁰⁴ (Reprinted with permission from ref 9. Copyright 1988.)

the methyl group of propene and the atoms of the growing chain. For a C_s symmetric catalyst such as $\{[{}^i\text{Pr}(\text{CpFlu})\text{HfCl}_2]$, the authors furthermore showed that opposite enantiofaces are preferred for (R) and (S) metal-propene complexes and noted that alter-

nation between the latter two during propagation would explain the formation of a syndiotactic polymer.

Utilizing the above-described π complex modeling approach, or slight variations thereof, Guerra, Cavallo, and Corradini et al. have later performed a series of investigations^{26–41} covering a number of different aspects of homogeneous transition metal catalyzed polymerization, including regiocontrol^{33,34,39,41} and back-skip.^{34,38} Throughout the years, they gradually increased the number of geometry variables actually optimized in the molecular mechanics calculations. In their 1997 investigation of the relationship between regioselectivity and type of stereospecificity,³⁹ only parameters pertaining to the coordination of the olefin were fixed.

To increase the flexibility in the geometry optimization procedure was also a central motivation behind the contributions of Angermund and Fink et al.^{42,43} Augmenting the Tripos force field⁴⁴ in order to incorporate handling of coordination of carbon-bridged ancillary ligands through a centroid approach (involving a dummy atom at the center of each η^5 -bonded ligand as further described in ref 43), the structure of a series of the thus formed zirconocene dichlorides could be optimized without constraints to good agreement with crystal structures.⁴² Later, they applied this force field to π complexes of the corresponding alkyl cations⁴³ for stereospecific olefin polymerization. They demonstrated how such complexes could be fully optimized in order to give relative energies of the four diastereomers (*Rre*, *Rsi*, *Sre*, and *Ssi*) that were in good qualitative agreement with the microstructure of the polymer obtained. For example, increasing the size of the substituent R in $\{[{}^i\text{Pr}(3\text{-RCpFlu})\text{ZrCl}_2]$ results in energetical separation of *Sre* and *Ssi* as seen in Figure 3. With R = ^tBu, (R) and (S) metal complexes prefer propene coordination with identical facial orientation (*re*), the calculations clearly predicting formation of isotactic polymer as experimentally obtained.

III. Combined QM/MM Approaches

There are several problems connected to the use of π complex models in the studies of specificity for α -olefin insertion. First, a correct description of alkenes weakly coordinated to d^0 metals of group IV [as opposed to those with a Dewar-Chatt-Duncanson metal-alkene bond^{45,46} as for Ti(II)-alkene compounds¹⁶] is difficult to achieve through a force field approach, although progress in the synthesis and characterization of d^0 metal-olefin complexes^{47–49} may enable parametrization of improved force fields specifically aimed at treating such complexes. Second, assuming a reversible olefin insertion, the stereospecificity of a catalyst should ultimately be determined at the transition state (TS) of this reaction step and one might fear that results obtained using π complex models are not accurate enough. Several researchers have thus sought to incorporate structural information from quantum chemical studies in investigations of stereoregulation.

A series of quantum chemical studies of ethylene insertion using catalysts based on early transition metals have contributed to our current understand-

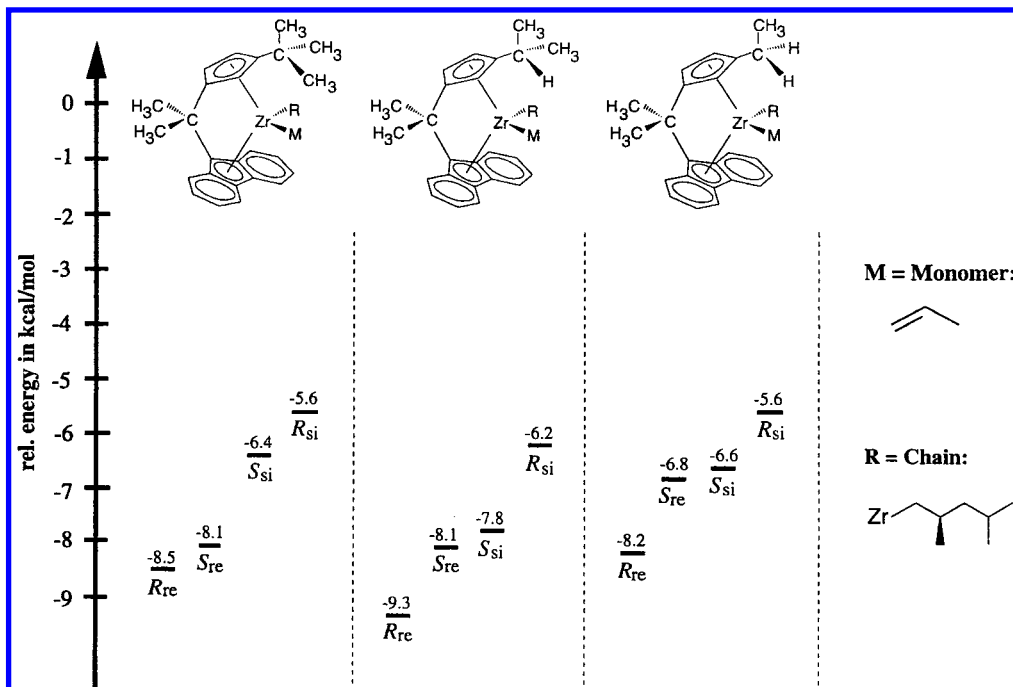


Figure 3. Energy differences between the diastereomers of various $[1\text{-Pr}(3\text{-RCpFlu})\text{Zr}(\text{propene})(2,4\text{-dimethylpentyl})]^+$ complexes. (Reprinted with permission from ref 43. Copyright 1997.)

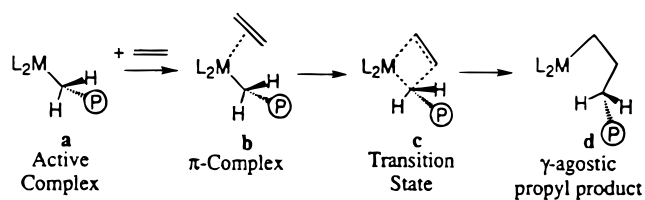


Figure 4. Schematic representation of Cossée-Arlman type reaction mechanism for homogeneous polymerization with metallocene-based catalysts.¹⁰⁴ (Reprinted with permission from ref 51. Copyright 1994.)

ing of the polymerization mechanism, see, e.g., refs 50–56. The general impression from these studies is that the direct, migratory insertion mechanism proposed by Cossée and Arlman^{4–6} (see Figure 4) almost 40 years ago is confirmed to represent a very reasonable reaction path for the propagation, subject to some additional refinement.

The barrier to insertion through a four-center TS is found to be very low, typically below 5 kcal/mol, and it is thus not likely that the regular back-skip of the growing polymer chain proposed by Cossée and Arlman can compete with consecutive insertions from alternating coordination sites as the main mechanism of propagation at ambient temperatures and reasonable monomer concentrations. The theoretical studies have also pointed out the important role that the different metal–H agostic interactions play at virtually all stages of the catalytic reaction. For example, an α -H agostic interaction is invariably found at the four-center TS of olefin insertion as evident from the quantum chemically optimized transition-state structures in Figures 5, 6, and 7 and seems to be important for stabilizing the structures in the transition region as well as for restricting the conformational freedom resulting from rotation around the metal–polymer bond.

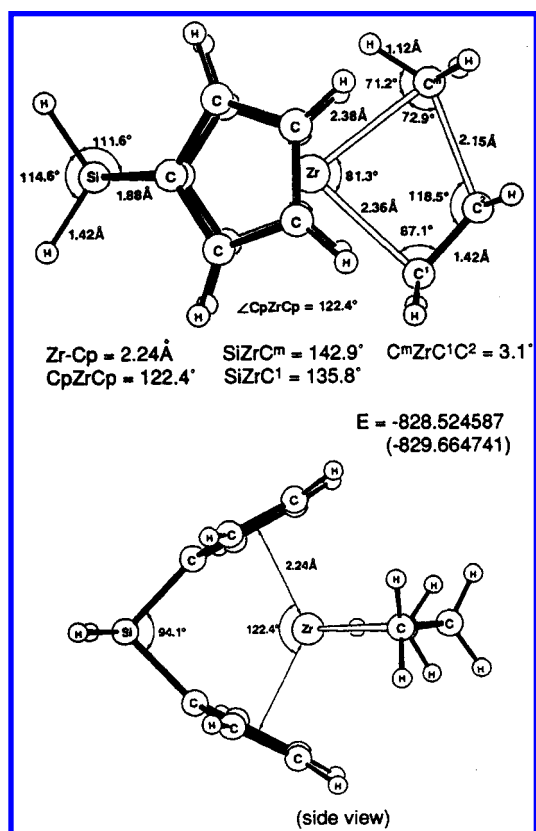


Figure 5. Hartree-Fock optimized TS for ethylene insertion into the Zr–CH₃ bond in $[\text{H}_2\text{Si}(\text{Cp})_2\text{Zr}-\text{CH}_3]^+$.¹⁰⁴ (Reprinted with permission from ref 64. Copyright 1992.)

Inclusion of the agostic metal–H bond may thus be of particular importance for studies of stereocontrol since the presence of this bond forces the second carbon atom of the polymer chain into a position which ensures some repulsive interaction with one of the ancillary ligands as seen for the two nonagostic hydrogens of the methyl group at the TS of ethylene

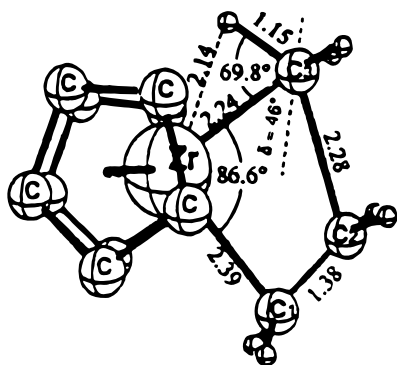


Figure 6. DFT optimized TS for ethylene insertion into the Zr-CH₃ bond in [(Cp)₂Zr-CH₃]⁺.¹⁰⁴ (Reprinted with permission from ref 51. Copyright 1994.)

insertion in Figure 5. Within the π complex model (no agostic hydrogen), exclusion of metal-polymer rotamers not offering significant steric discrimination^{9,23-41} has been based on principles of “least nuclear motion”.¹⁷⁻¹⁹ The presence of an α -agostic interaction at the TS has been confirmed in isotopic-labeling experiments by Krauledat and Brintzinger.⁵⁷

On the basis of ab initio investigations of ethylene insertion into the [Cl₂Zr-CH₃]⁺ bond, Rappé and co-workers⁵⁸⁻⁶¹ introduced an “activated complex” (AC) to be used in molecular mechanics investigations of stereospecificity of propene insertion for a series of metallocene-based catalysts. The AC (Figure 8) was defined as an assumed point on the reaction path of propene insertion, located roughly halfway between the π complex and the TS of insertion as determined in the ab initio studies of ethylene insertion for the small model system.

For the AC, identical Zr-C distances (2.5 Å) were adopted for the sp² carbons of the ethylene in addition to a relatively long (2.9 Å) forming carbon-carbon

bond, leaving the AC with a strong π complex character. Rappé and co-workers extended the Dreiding force field⁶² to include, among other, a centroid approach for describing Zr-Cp bonds and arrived at a model allowing for complete geometry optimization. Their calculations showed in general a good, qualitative agreement between experimentally and theoretically determined tacticity and also allowed for predictions of catalyst modifications for improvement of specificity. However, application of the AC approach to the (known) syndiospecific catalyst [(Pr(CpFlu))Zr-CH₃]⁺⁵⁸ resulted in a serious deviation from experiment. For the third insertion of propene, the AC leading to an isotactic defect was favored by about 2 kcal/mol compared to the complex leading to syndiotactic polypropene.

In 1992, Morokuma et al.⁶³ performed an ab initio study of ethylene insertion into the metal-methyl bond in [Cl₂Ti-CH₃]⁺. Replacing one of the ethylene hydrogen atoms by a methyl group, they used the π complex and transition-state geometries as determined for the ethylene insertion reaction in the ab initio investigation of propene insertion for this small model complex. Although the stereospecificity for this achiral model catalyst in itself is not very interesting, they pointed out that the observed tendency of the four-center transition state to adopt a nonplanar geometry may be of importance for catalysts with chain-end stereocontrol (i.e., stereochemical control mainly through the orientation of the last inserted unit).

Using molecular mechanics for the study of propene insertion, they extended their investigations to a series of silylene-bridged metallocenes.^{64,65} The transition-state structures used in the MM investigations were taken from ab initio studies of ethylene insertion for the corresponding unsubstituted com-

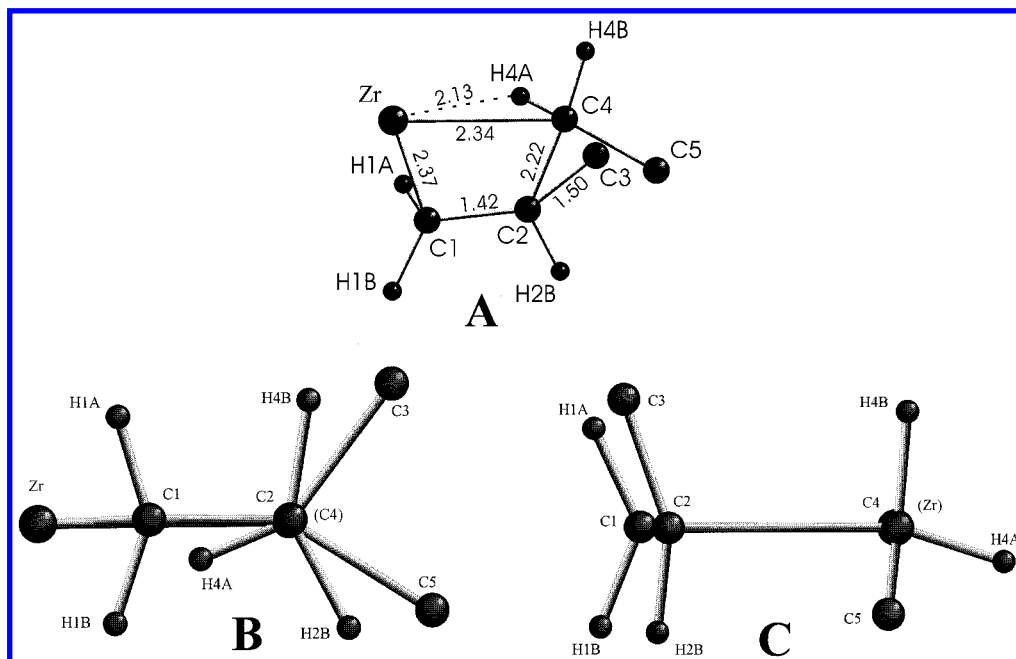


Figure 7. The 11-atom aggregate (panel A with distances in angstroms) obtained from a DFT-based geometry optimization of [(CH₂(Cp)₂)Zr-^tBu]⁺ as performed in ref 70. Due to the two possible coordination faces of propene the aggregate was applied as shown for *si* complexes and in the inverted form when studying *re* complexes. (B) View along axis C2-C4. (C) View along axis C4-Zr.

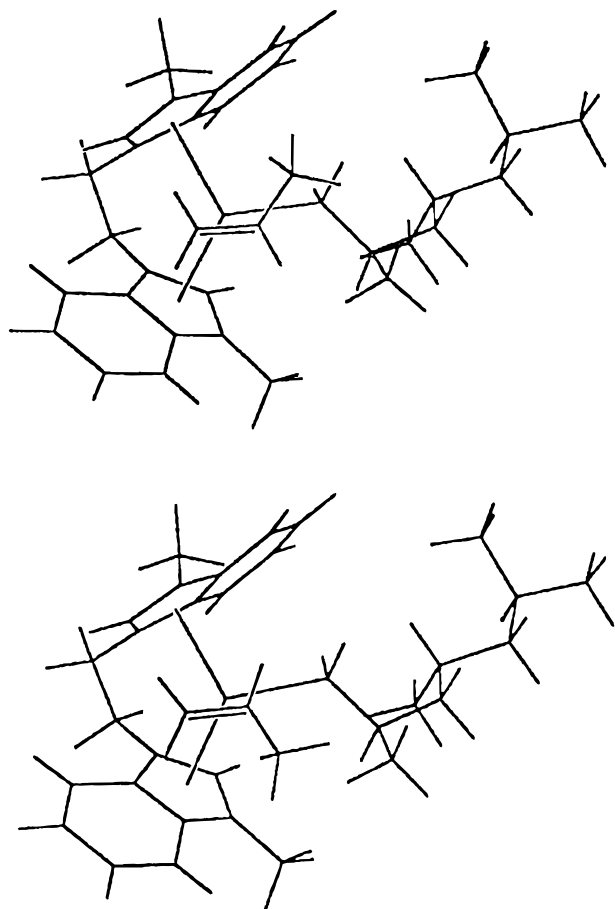


Figure 8. Activated zirconocene complex leading to isotactic insertion (top) and syndiotactic defect (bottom).¹⁰⁴ (Reprinted with permission from ref 59. Copyright 1993.)

plexes with one of the hydrogens replaced by a methyl group. For example, in the investigation of regio- and stereoselectivity of various methyl-substituted bis(Cp) catalysts, $[\{H_2Si(CpMe_n)_2\}Zr-CH_3]^+$,⁶⁴ only the methyl groups of propene and the substituents on the cyclopentadienyl ligands were geometry optimized in the MM calculations. The rest of the geometry was fixed to that determined by ab initio (Hartree-Fock) for ethylene insertion into the metal-methyl bond in $[\{H_2Si(Cp)_2\}Zr-CH_3]^+$ (Figure 5), thus preserving important structural features such as the α -agostic metal-H bond.

The MM optimizations were performed using the MM2 force field^{66,67} with the metal treated as a dummy atom having zero force constants. They were able to separate their calculated energy differences (termed steric energies) into a direct (caused by catalyst-olefin interactions) and an indirect part (caused by interactions between olefin and the growing polymer chain) and generally concluded that stereocontrol mainly is governed by the indirect interaction term. Their calculated regioselectivities using π complex geometries were at variance with those obtained using TS geometries⁶⁴ and the authors stressed the importance of using reasonable TS structures for comparison of steric energies. In their comparison of different metals, they pointed out that, due to the smaller atomic radius giving tighter and sterically more discriminating transition states, titanium-based catalysts should have a higher intrinsic

ability for stereocontrol than zirconium- and hafnium-based analogues.⁶⁵ They were furthermore able to obtain good discrimination between the predicted stereoregulating abilities of various ligands, and the predictions were in line with experiment. They reported the asymmetric catalyst $[\{H_2Si(3\text{-}t\text{-Bu-CpFlu})\}Zr-R]^+$ to be among the best with respect to stereoregulating abilities. The isospecificity of this catalyst claimed to be the result of blocking of one of the two sites [(R) or (S), originating from the fact that the metal is a stereogenic center] by the *tert*-butyl substituent. Highly isotactic polymer is thus obtained as insertion takes place only from the site for which insertion is not blocked, and this site has a clear enantioselectivity with respect to the coordination face of propene through indirect control: the chain is oriented so as to avoid repulsive interaction with the fluorenyl ligand and this orientation is decisive for the choice of propene coordination face.

In 1995, Chien and Yu^{68,69} used the π complex and TS structures of ethylene insertion into the metal-methyl bond in $[\{H_2Si(Cp)_2\}Zr-CH_3]^+$ (Figure 5) as optimized by Morokuma et al.⁶⁴ for the study of regio- and stereospecificity of propene insertion for several ansa-metalloenes. They replaced one of the ethylene hydrogen atoms by a methyl group and fixed all bond distances and valence angles pertaining to the four-membered metal-ethylene-methyl ring in all MM calculations. By constraining various metal-H-C distances to values obtained by Morokuma et al., they also included effects of different metal-H agostic interactions in some of the calculations. With an augmented MM2 force field^{66,67} and by replacing one ethylene hydrogen by a methyl group as well as using various alkyl groups as a model for the growing polymer chain P, they calculated the steric energies of propene insertion for the isospecific catalysts $rac\text{-}[\{C_2H_4(Ind)_2\}Zr-P]^+$ and $rac\text{-}[\{C_2H_4(H_4Ind)_2\}Zr-P]^+$ ⁶⁸ and later applied the same approach to the study of syndiospecific polymerization using $[\{t\text{-BuHC}(\text{CpFlu})\}Zr-P]^+$ and $[\{Pr(\text{CpFlu})\}Zr-P]^+$.⁶⁹ Both iso- and syndiospecificities were found to increase significantly (~ 0.7 kcal/mol) through introduction of an α -agostic metal-H bond at the TS. With such a bond present, isoselectivities were found to be slightly higher than for the corresponding fixed π complex model, the results from both approaches, however, being in good agreement with the fact that the two C_2 -symmetric complexes are highly isospecific catalysts. On the other hand, a satisfactory regioselectivity was only obtained using the TS structures. Furthermore, $[\{t\text{-BuHC}(\text{CpFlu})\}Zr-P]^+$ was found to be slightly more syndiospecific than $[\{Pr(\text{CpFlu})\}Zr-P]^+$, in agreement with experiment. On the basis of their calculations, Chien and Yu also claimed that the *mm* triad defect in syndiotactic polymer mainly is caused by insertion of propene units with the wrong facial orientation and does not result from back-skip.

Guerra and Cavallo et al.^{37,41} obtained the coordinates of atoms involved in forming and breaking of bonds (the four-membered metal-ethylene-methyl ring) from a TS of ethylene insertion optimized by Ziegler et al.^{50,51} (Figure 6) using density functional

Table 1. Important Geometric Parameters (Å, deg) and Relative Energies of DFT-Optimized Transition States of Propene Insertion

geometry parameter	$[\{\text{CH}_2(\text{Cp})_2\}\text{Zr-}^i\text{Bu}]^+$	$[\{\text{CH}_2(\text{CpInd})\}\text{Zr-}^i\text{Bu}]^+$		$[\{\text{CH}_2(3\text{-Me-CpCp})\}\text{Zr-}^i\text{Bu}]^+$	
	<i>re/si</i>	<i>Rre</i>	<i>Rsi</i>	<i>Rre</i>	<i>Rsi</i>
Zr–C1	2.37	2.36	2.38	2.35	2.37
Zr–C4	2.34	2.33	2.33	2.35	2.35
C1–C2	1.42	1.42	1.42	1.43	1.42
C2–C4	2.22	2.23	2.27	2.18	2.23
$\angle\text{ZrC4C5}$	147.9	150.1	153.4	148.1	153.4
$\angle\text{ZrC1C2C4}$	–0.5/0.5	2.3	–1.9	–1.3	–1.8
energy ^a		0	2.8	0	2.9

^a For the two catalysts with a stereogenic metal center the energy (kcal/mol) is given relative to the most stable (R) diastereomer.

theory (DFT). In their 1996 study of doubly bridged zirconocenes³⁷ they also constrained ϑ_1 (defined in Figure 2) to -83° and $+83^\circ$ for *re* and *si* coordination of propene, respectively, whereas, in their recent study of the effects of ancillary ligand substitution,⁴¹ they allowed a maximum of $\pm 15^\circ$ change in torsional angles involving the atoms for which the structure was taken from DFT. Although not explicitly fixing an agostic metal–H bond in the MM investigations, it is likely that both of these approaches to some extent preserved the orientation of the second carbon atom of the polymer chain that would arise from an α -agostic metal–H bond. In these studies, the authors also employed their π complex approach as described in a previous section. Comparison of the results obtained using the π complexes with those derived using a fixed TS geometry indicate significant differences in the relative energies, although the qualitative trends usually remain unchanged.^{37,41}

We have seen that several studies have been based on approaches involving fixing the coordinates of a central part (termed “aggregate”) of the transition-state structure,^{37,41,58,59,64,65,68,69} although the validity of this approximation has never been checked. The assumption that the coordinates of the aggregate can be kept identical in molecular mechanics investigations of a wide range of catalysts is based on the idea that the four-center metallacycle-like TS should remain relatively constant as long as the metal atom and its first coordination sphere are left unchanged. A constant central part, however, undoubtedly introduces an error to the calculations. For example, in the force field calculations, the aggregate is not allowed to respond to the introduction of a substituent on the ancillary ligands. All such relaxation must be accounted for by geometrical variables outside the aggregate, and a priori, one should therefore expect the thus calculated energy differences to be overestimated.

The apparent lack of quantitative information about the effects of applying aggregates prompted us to investigate this matter ourselves. The selected aggregate was obtained from a DFT-based geometry optimization of $[\{\text{CH}_2(\text{Cp})_2\}\text{Zr-}^i\text{Bu}]^+$ and encompassed 11 atoms as shown in Figure 7 and whose Cartesian coordinates are given in ref 70. Due to the two possible coordination faces of propene (*re* and *si*), the aggregate was applied as shown in Figure 7 for *si* complexes or in the inverted form when studying *re* complexes. DFT geometry optimization was performed using the BPW91-functional^{71–73} together

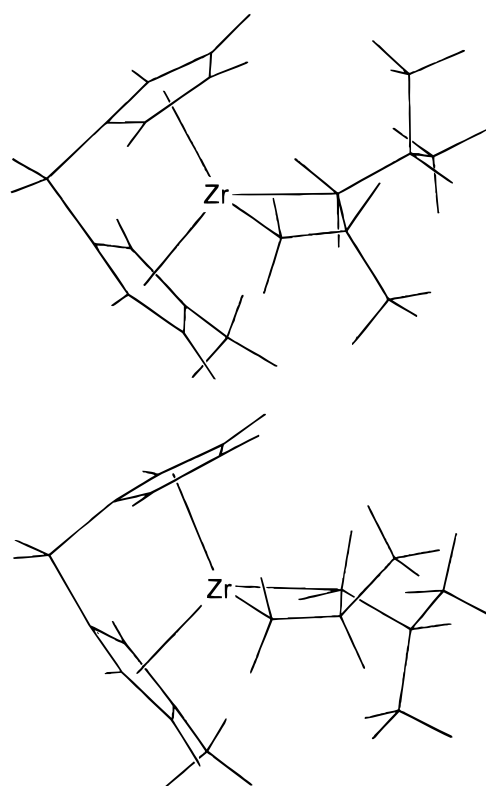


Figure 9. DFT optimized transition states of propene insertion into the zirconium-isobutyl bond in $[\{\text{CH}_2(3\text{-Me-CpCp})\}\text{Zr-}^i\text{Bu}]^+$. Upper structure, *Rre* lower structure, *Rsi*.

with Slater-type bases^{74,75} of triple- ζ (Zr), double- ζ plus polarization (C and H atoms belonging to the monomer or the polymer chain), and double- ζ (all other atoms) quality. The calculations were performed within the frozen core approximation using the program system ADF.^{76–78} Further computational details can be found in ref 70.

To investigate to what extent modifications of the ancillary ligand result in geometric changes in the central aggregate region, *Rre* and *Rsi* diastereomeric transition states of propene insertion were optimized using DFT for both $[\{\text{CH}_2(\text{CpInd})\}\text{Zr-}^i\text{Bu}]^+$ and $[\{\text{CH}_2(3\text{-Me-CpCp})\}\text{Zr-}^i\text{Bu}]^+$ catalytic complexes. Important geometric parameters from these complexes as well as from $[\{\text{CH}_2(\text{Cp})_2\}\text{Zr-}^i\text{Bu}]^+$ are given in Table 1 and the two (R) diastereomers of the methyl-substituted catalyst are displayed in Figure 9.

The transition states of insertion are all located close to the midpoint of the reaction coordinate as judged from the forming Zr–C bonds being equal to or slightly longer than those being broken. The

α -agostic interaction usually found at the TS in quantum chemical studies of metal-catalyzed alkene insertion is present in all the complexes, with a lengthening of the C–H bond of 4–5 pm. The four 11-atom central geometries from the two larger complexes are similar to the corresponding aggregates from the unsubstituted $\{[\text{CH}_2(\text{Cp})_2]\text{Zr}-\text{Bu}\}^+$ (Figure 7), with RMS deviations below 0.04 (0.06) Å for the *re* (*si*) aggregates. The exact position of the TS on the reaction coordinate (shortening of the C2–C4 bond) is seen to be dependent on the ancillary ligand, with calculated C2–C4 bonds varying from 2.18 to 2.27 Å. Although significant in terms of geometrical change, the DFT energy is seen to stay constant within ± 0.1 kcal/mol through 10 pm intervals of the C2–C4 bond length in the transition region. A probably more important difference between the aggregates obtained with and without a C_s symmetric ancillary ligand is the position of the second carbon atom of the polymer chain, i.e., C5. The *si* enantiofaces bring about a larger repulsive interaction between the indenyl or the Me-Cp ligand and the polymer chain, resulting in the latter being oriented somewhat more away from the former. The effect is seen as an opening of the ZrC4C5 angle and the H2BC2C4C5 torsion in cases where ligand-polymer chain repulsion is important, amounting to 4–5° compared to $\{[\text{CH}_2(\text{Cp})_2]\text{Zr}-\text{Bu}\}^+$. Unsymmetrical substitution of the ancillary ligand also results in the central four-membered metallacycle-like TS departing from the almost planar configuration seen for $\{[\text{CH}_2(\text{Cp})_2]\text{Zr}-\text{Bu}\}^+$ where the ZrC1C2C4 torsion is close to zero. This torsion, however, stays within $\pm 2^\circ$ also for the substituted complexes and a clear relationship between the propene coordination face and the value of the ZrC1C2C4 torsion does not exist. It should be noted that, although the zirconium atom, C1 and C2 of propene, together with the first atom of the polymer chain (C4) are almost located in a plane, the propene–polymer chain conformation is not eclipsed, as evident from the H2BC2C4C5 torsion being close to 30°. It is not clear as to what extent a staggered monomer–alkyl conformation could be realized in the studies where aggregate structures were taken from quantum chemical investigations of ethylene insertion.^{37,41,58,59,64,65,68,69}

Although it is gratifying that the geometric effect on the 11-atom central geometry resulting from substitution of the ancillary ligand is limited, it remains to be seen to what extent the use of a constant aggregate influences the relative energies. DFT geometry optimizations employing the frozen aggregate geometry from the unsubstituted bis(Cp) complex were thus performed for the (R) diastereomeric TS structures for $\{[\text{CH}_2(\text{CpInd})]\text{Zr}-\text{Bu}\}^+$ and $\{[\text{CH}_2(3\text{-Me-CpCp})]\text{Zr}-\text{Bu}\}^+$, enabling a direct comparison with the energies for fully optimized structures given in Table 1. Using the aggregate, the *Rre* complexes come out 2.5 and 2.7 kcal/mol more stable than the *Rsi* counterparts, i.e., with a $\Delta E = E(\text{Rsi}) - E(\text{Rre})$ for the enantioselectivity underestimated by 10 and 7%, respectively. Since the geometric deviation from the “ideal” aggregate in $\{[\text{CH}_2(\text{Cp})_2]\text{Zr}-\text{Bu}\}^+$ was found to be larger for the high-energy (*Rsi*)

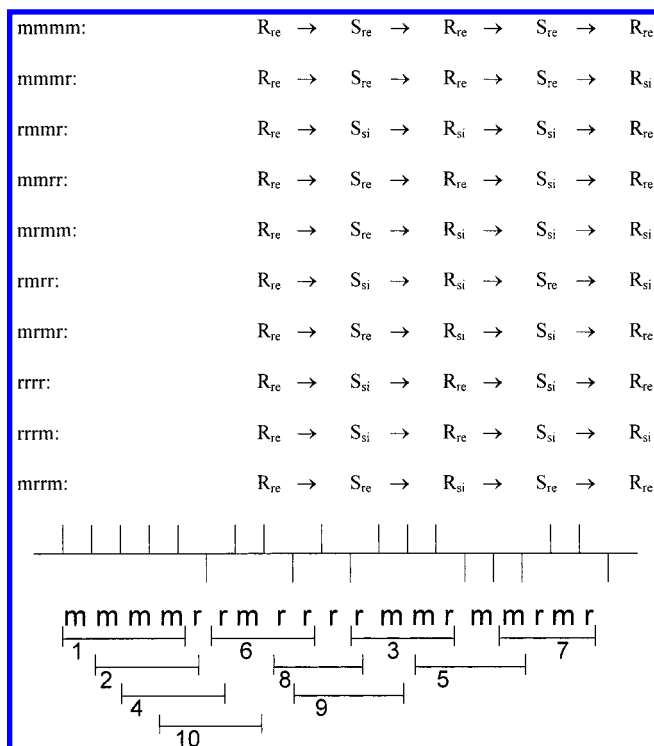


Figure 10. (Top) Sequences of configurations starting with *Rre* involved in generation of the various pentads. (Bottom) Ten possible pentads of polypropene. The number *n* of a pentad refers to the *n*th sequence of configurations. (Reprinted with permission from ref 43. Copyright 1997.)

diastereomers, it is somewhat surprising that the use of this aggregate results in underestimation of the enantioselectivity. However, a systematic error in the absolute energy differences introduced by the use of an aggregate is not problematic and it is far more important that the ratio between the enantioselectivity obtained for different catalysts seems to be maintained when using the aggregate.

IV. From Energy Differences to Pentad Distributions

In 1993, Hart and Rappé⁵⁹ realized that calculated energy differences between activated complexes (AC) of propene insertion can be converted to pentad intensities to be compared with corresponding intensities from NMR spectra.^{79–82} The intensities of the 10 possible pentads shown in Figure 10 are a common measure of the tacticity of the polymer. A given pentad intensity is the ratio of the corresponding pentad integral to the integral sum of all pentad signals observed and usually given in units of percent. Isotactic (syndiotactic) polymer is thus characterized by a high intensity for the *mmmm* (*rrrr*) pentad. The difference in free energy of activation [$\Delta\Delta G^\ddagger = \Delta G^\ddagger(\text{si}) - \Delta G^\ddagger(\text{re})$] between two competing reactions (here taken as an insertion for the *si* and *re* enantioface, respectively) is approximated by the MM calculated energy difference (ΔE) between to ACs and related to the corresponding rate constants k_{si} and k_{re} through eq 1.

$$\Delta E = -RT \ln \left(\frac{k_{\text{si}}}{k_{\text{re}}} \right) \quad (1)$$

In other words, applying Maxwell–Boltzmann statistics (see, e.g., ref 83 for a general treatment) to the calculated energy differences leads to estimated probabilities of obtaining *re* and *si* insertion (eq 2).

$$\rho_{si} = \frac{e^{-E_{si}/RT}}{e^{-E_{si}/RT} + e^{-E_{re}/RT}} = \frac{1}{1 + e^{\Delta E/RT}} \quad (2)$$

Considering each insertion as an independent event (which implies enantiomeric site control, i.e., the chirality of the catalyst is the dominating factor for stereocontrol), Hart and Rappé⁵⁹ then calculated the intensities for the *mmmm* pentad by multiplication of the individual probabilities. The calculated intensities were in excellent agreement with those from NMR data for a series of substituted ethylene-bridged, C_2 -symmetric zirconocenes. The use of this new and more quantitative approach to analysis of the relationship between the molecular structure of the catalyst and the polymer microstructure was, however, restricted to comparison of intensities for the *mmmm* pentad. Application to error pentads or prediction of pentad distributions for new or modified catalysts was not attempted.

A couple of years later, calculation of complete pentad distributions was performed by Chien and Yu in their MM investigations of isospecific⁶⁸ and syndiospecific⁶⁹ polymerization using ansa-zirconocenes. Pentad distributions were calculated at several temperatures using two different stereochemical control models, one implying enantiomeric site control and the other chain-end control (i.e., the orientation of the last inserted unit is determining). For each catalyst and polymer fraction (depending on the solvent used for extraction), they scaled the MM steric control energy to give a pentad distribution showing the best possible fit with the corresponding experimentally obtained distribution. For isospecific polymerization using *rac*-[$\{C_2H_4(H_4Ind)_2\}Zr-P]^+$ the enantiomeric site control model was found to afford the best agreement with experiment, whereas for syndiospecific polymerization with [$\{^iBuHC(CpFlu)\}Zr-P]^+$, the calculations indicated that enantiomeric site control is operative at lower and chain-end control at higher temperatures. In the case of isospecific polymerization, both approaches gave pentad distributions in impressive agreement with experiment, the intensity for the *mmmm* pentad being reproduced to within a few tenths of a percentage point in both cases. Nevertheless, the use of separate scaling for each catalyst fraction makes the predictive abilities of the approach taken seem rather slim if aimed at calculating pentad distributions of new or modified catalyst structures.

V. Systematic and Independent Prediction of Pentad Distributions

Recently, an attempt at going beyond the qualitative classification of catalysts through calculated enantioselectivities was made for a series of catalysts displaying varying stereospecificities.⁷⁰ The computational approach was based on the simplest possible combination of quantum chemistry and molecular

Table 2. Relative MM Energies (kcal/mol) of the Most Stable Conformers of the Four Diastereomeric Models of the TS of Propene Insertion for Catalysts 1–9

compd	Rre	Rsi	Sre	Ssi
1	0.00	1.99	1.99	0.00
2	0.00	2.03	0.00	2.03
3	0.00	1.39	0.12	0.02
4^a	0.00	2.34	2.23	1.45
5^a	0.00	2.28	1.84	1.25
6^a	0.00	2.39	1.32	1.30
7	0.00	2.81	0.53	4.34
8	5.98	0.00	5.98	0.00
9	0.83	6.91	0.00	6.71

^a The pentad intensities for compounds **4–6** (Table 4) were obtained from Boltzmann distributions also involving energy levels of higher-lying conformers (see ref 70 for details).

mechanics (MM): the geometry of the central part where bond breaking and bond forming takes place (termed aggregate) was first optimized in a separate density functional theory calculation and later used “as is” in a series of force field-based calculations.

The propagation was considered to proceed with unbroken alternation between (S) and (R) complexes. Thus, (S) and (R) complexes were regarded as kinetically separated which implies that no back-skip occurs. The treatment was also limited to encompassing stereospecificity only, i.e., regiospecificity was not included.

Gibbs free energies of the four diastereomeric transition states of insertion, *Rre*, *Rsi*, *Sre*, and *Ssi*, were approximated by the corresponding MM energies (Table 2), Boltzmann distribution⁸³ between the enantiofaces (*re* and *si*) was realized for every insertion, and each insertion was considered to occur independently of the other in accord with the enantiomeric site control model. When comparing with the probability of a particular pentad as obtained from an NMR spectrum, one then simply needs to consider the four five-membered sequences of transition states leading to this pentad. The sequences starting with *Rre* are shown in Figure 10.

Finally, the theoretical pentad probability is given as the sum of each individual sequence probability, renormalized (divided by two) in case of symmetric pentads (*mmmm*, *rrrr*, *mrrm*, and *rmmr*).

The molecular mechanics calculations were performed with the SYBYL program⁸⁴ using an extended⁴² and reparametrized⁷⁰ Tripos force field.⁴⁴ The reparametrization attempted to reproduce geometries and in part also relative energies of transition structures of propene insertion for various methylene-bridged zirconocenes as obtained with DFT and was performed to account for the presence of the aggregate. Furthermore, the coordinates of the aggregate were fixed, no point charges were used, and the cutoff for nonbonded interactions was set to 12 Å.

Four of the catalysts presented in Figure 11 contain unsubstituted cyclopentadienyl, indenyl, or fluorenyl ligands. Of these, **1**, **2**, and **3** represent well-known examples of catalysts producing syndiotactic, isotactic, and hemiisotactic polypropene at low temperatures, respectively, and we will thus start our analysis of the theoretically derived pentads by comparing

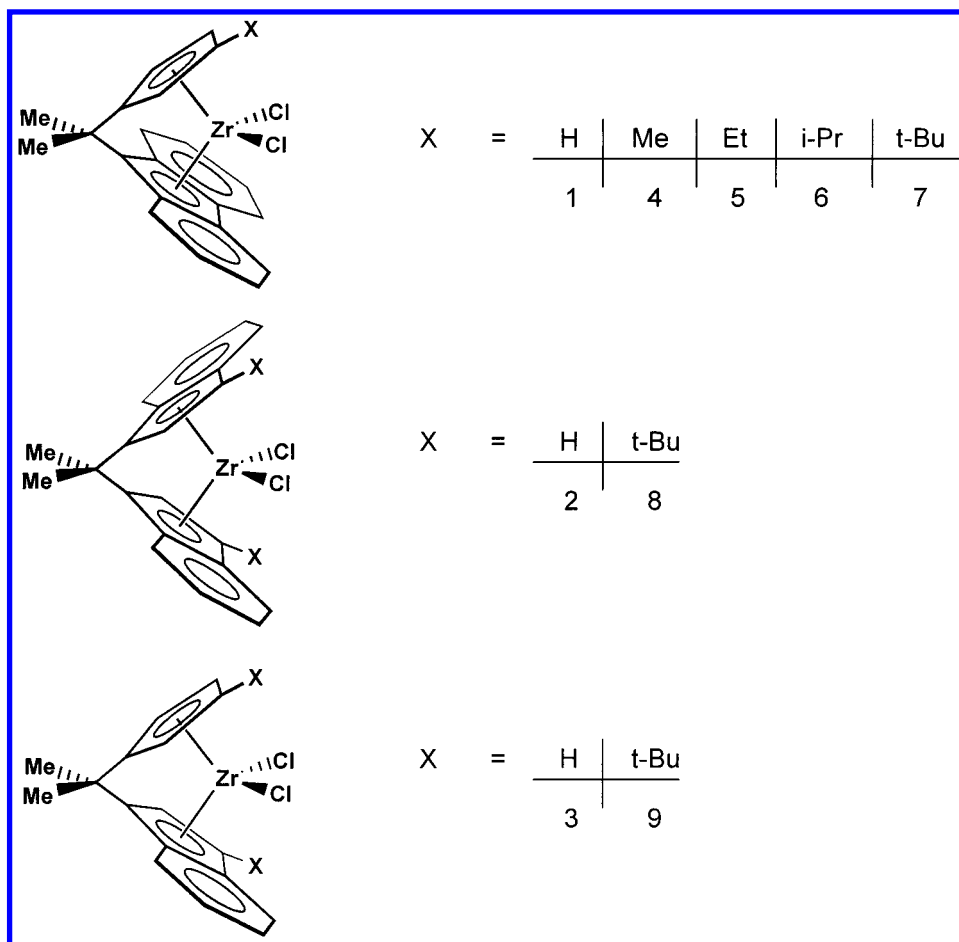


Figure 11. Structures of *ansa*-zirconocenes discussed in sections V and VI. **1**, [$\{\text{Pr}(\text{CpFlu})\}\text{ZrCl}_2$]; **2**, *rac*- $\{\{\text{Pr}(\text{Ind})_2\}\text{ZrCl}_2$]; **3**, [$\{\text{Pr}(\text{CpInd})\}\text{ZrCl}_2$]; **4**, [$\{\text{Pr}(3\text{-MeCpFlu})\}\text{ZrCl}_2$]; **5**, [$\{\text{Pr}(3\text{-EtCpFlu})\}\text{ZrCl}_2$]; **6**, [$\{\text{Pr}(3\text{-PrCpFlu})\}\text{ZrCl}_2$]; **7**, [$\{\text{Pr}(3\text{-BuCpFlu})\}\text{ZrCl}_2$]; **8**, *rac*- $\{\{\text{Pr}(3\text{-BuInd})_2\}\text{ZrCl}_2$]; **9**, *threo*- $\{\{\text{Pr}(3\text{-BuCp-3-BuInd})\}\text{ZrCl}_2$].

Table 3. Calculated (Observed) Pentad Distributions (%) of Polypropene Obtained from Polymerization Using Catalysts 1–3

compd	temp (°C)	[<i>mmmm</i>]	[<i>mmm</i> r]	[<i>rmm</i> r]	[<i>mmrr</i>]	[<i>rrmm</i>] + [<i>rrmr</i>]	[<i>mrr</i> r]	[<i>rrrr</i>]	[<i>rrrm</i>]	[<i>mrrm</i>]	RMS dev ^a
1	10	0(0)	0(0)	3(1)	5(2)	0(1)	0(0)	87(93)	5(3)	0(0)	1.6
	50	0(0)	0(0)	4(2)	7(3)	1(5)	0(0)	80(83)	7(8)	0(0)	1.6
	70	0(0)	1(2)	4(2)	8(5)	1(12)	1(3)	77(59)	8(18)	0(0)	5.3
2	10	88(83)	5(8)	0(0)	5(6)	0(0)	0(0)	0(0)	0(0)	2(4)	1.2
	30	84(81)	6(9)	0(0)	6(7)	0(0)	0(0)	0(0)	0(0)	4(4)	1.1
	50	81(68)	7(16)	0(0)	7(11)	0(0)	0(0)	0(0)	0(0)	3(6)	3.3
3	−30	13(19)	11(18)	7(4)	22(22)	5(10)	3(2)	20(7)	14(8)	6(11)	5.3
	10	12(19)	11(19)	7(3)	21(22)	7(13)	4(4)	18(6)	14(6)	6(8)	5.2
	50	12(9)	11(15)	7(5)	20(17)	9(20)	5(7)	17(7)	14(11)	6(9)	4.3

^a In percentage points, calculated using pentad intensities including one value after the decimal point.

with the experimentally obtained pentads for the latter three as given in Table 3. In the following, all pentad intensities are given in units of percent and symbolized by using square brackets: the degree of isotacticity (the intensity for the *mmmm* pentad), for example, will be designated by [*mmmm*].

At low temperatures, the calculated pentad distributions for **1** and **2** are in excellent agreement with experiment, with overall RMS deviations at 10 °C amounting to 1.6 and 1.2 percentage points, respectively. The theoretical pentad distribution for **1** reflects slightly less syndiospecificity than found in analysis of the ¹³C NMR spectrum, whereas **2** along with the related, sterically more encumbered catalyst **8**,⁸⁵ is predicted to be somewhat too isospecific. The

latter has a calculated (measured) [*mmmm*] of 100 (97)% at 20 °C. However, these deviations are minor, and it is gratifying that not only the highest peaks (*mmmm* and *rrrr*) in the NMR spectra are reproduced but that also the type and relative size of the stereoerrors are accurately predicted. For example, for **2**, *mmm*r, *mmrr*, and *mrrm* are the polymer pentads reflecting the stereoerrors compared to ideal isotactic polypropene. The theoretical error pentads appear in the 2:2:1 ratio expected for catalytic site control, which also is the pattern roughly displayed by the experimental pentads. To conclude, at low temperatures, it is possible to calculate the magnitude of the specificity (given as the intensities for *mmmm* and *rrrr*) with very good accuracy as well as

the qualitatively correct pattern associated with pentads arising from stereoerrors. The predictions are also accurate at intermediate temperatures (30–50 °C), which means that reduction in specificity for these catalysts along with rising temperature can be explained by simple Maxwell–Boltzmann statistics: stereoerrors occur when the insertion passes through a TS with wrong (i.e., *si* instead of *re*) enantiofacial orientation of propene and an increasing fraction of the propene molecules will pass through such energetically higher-lying transition states with rising temperature.

Above 30–50 °C, however, it is clear that the reduction in specificity is more dramatic than that predicted by a Boltzmann distribution among the various diastereomers of propene insertion alone. For the syndiotactic catalyst **1**, the observed intensity for the *rrrr* pentad is reduced by 24 percentage points when going from 50 to 70 °C compared to only 3 obtained with the current modeling scheme. At elevated temperatures, it is conceivable that isomerization reactions, involving higher activation energies than that of the insertion, become increasingly important. For **1**, single *m* dyads are seen to be the most important type of stereoerror, and for a syndiospecific catalyst, the occurrence of such errors can best be explained^{86,87} by assuming back-skip. The importance of a significant barrier to chain migration in syndiospecific polymerization has also been pointed out in a theoretical study.⁸⁸ A back-skip can be viewed as an inversion of the catalytic center, i.e., instead of proceeding through a (S) transition state after completing insertion for a (R) complex, the chain migrates back to the position suitable for a second consecutive insertion through a (R) transition state. Improving the current model through inclusion of back-skip will require some estimate of the barrier to chain migration. For **2**, the large drop in [*mmmm*] that cannot be explained by the current method starts already between 30 and 50 °C and is accompanied by increasing intensities for the error pentads *mmmr*, *mmrr*, and *mrrm*. It has been noted that growing chain epimerization processes^{89,90} may become significant above ambient temperatures,^{91–93} and it seems reasonable to ascribe most of the difference between the observed temperature dependence and the Boltzmann-derived profile to such a side reaction which may lead to single, stereoinverted methyl groups detectable as *rr* triads. Leclerc and Brintzinger^{94,95} confirmed the existence of stereoinverted CH₂D groups resulting from of chain-end isomerization through detection of D-labeled *mrrm* stereoerrors in isotactic polypropene obtained during polymerization of (*E*) or (*Z*)-[D₁]-propene, although it is at present not clear why D-labels were not observed for the asymmetric pentads (*mmmr* and *mmrr*) associated with *rr* triads.

For **3**, the predicted pentad distribution is inaccurate (RMS deviations above 5 percentage points) even at low temperatures. This catalyst is normally referred to as hemiispecific, although the low intensities observed for the *rrrr* pentad suggest that “weakly isospecific” perhaps is a better term. With one olefin coordination site being ideally enantio-

selective and the other completely unselective, the occurrence of *mmmm* and *rrrr* pentads should be equal (18.8%), which is not far from being the case for the calculated pentads. The experimentally obtained pentads, on the other hand, show that the two sites [(R) and (S)] prefer insertion of propene with identical enantiofacial orientation. However, the enantioselectivity of insertion from (S)-diastereomers is weak, as is evident from the low observed isospecificity together with the fact that the *Ssi* and *Sre* complexes have very similar calculated energies. A tiny variation of the selectivity for this coordination site brings about marked changes in the pentad distribution. Calculations with the current approach predict that the *si* enantioface is more stable by about 0.1 kcal/mol, i.e., that the catalyst should produce polypropene with some syndiotactic character with a [*rrrr*] above 20%. A shift to 0.1 kcal/mol selectivity for the *opposite* enantioface would result in exchange of values between [*rrrr*] and [*mmmm*], in significantly better agreement (RMS deviation of <3 percentage points) with the slightly isotactic polymer actually obtained. In other words, in cases where the enantioselectivity is not clear, e.g., due to lack of steric demanding substituents, even small inaccuracies in the methodology can result in large errors in the calculated pentad distribution. The contrast to catalysts where the enantioselectivities are more pronounced becomes evident when considering the related catalyst **9**. The additional *tert*-butyl substituents ensures increased preference for the propene *re* enantioface affording a polymer almost without stereoerrors ([*mmmm*] ≈ 99% at 30 °C).⁹⁶ The calculated enantioselectivities (see Table 2) for this catalyst are somewhat overestimated, resulting in a predicted [*mmmm*] of 100% at 30 °C. It is conceivable that the deviations seen for compound **3** result from inaccuracies in the force field parameters. It is equally conceivable that reliable performance in such cases (low enantioselectivity) is very hard to obtain with molecular mechanics. At elevated temperatures, the small error in the calculated enantioselectivity for (S) complexes gradually loses importance. Already at 50 °C, the calculations predict that **3** produces atactic polymer, in accord with experiment.

Thus, for prime examples of catalysts of significant isospecific or syndiospecific character, it seems to be possible to calculate the pentad distribution independently with very good accuracy at low temperatures using a relatively simple molecular mechanics approach. For catalysts with weak enantioselectivities, small errors in the calculated selectivity may lead to marked errors in the predicted pentad distribution.

VI. Further Treatment of Temperature Effects

In ref 70, calculation of pentad distributions at different temperatures was performed with the specific aim of extracting mechanistic information. All the alkyl-substituted catalysts **4–7** (Figure 11) become increasingly isospecific with rising temperature. One possible explanation for this phenomenon is that the effective steric influence from the alkyl substituents is enlarged as energy levels of higher-lying

Table 4. Calculated (Observed) Pentad Distributions (%) of Polypropene Obtained from Polymerization Using Catalysts 4–7

compd	temp (°C)	[mmmm]	[mmmr]	[rmmr]	[mmrr]	[mrrmm] +					RMS dev ^a
						[rrmr]	[mrrr]	[rrrr]	[rrrm]	[mrrm]	
4	–30	4(13)	5(11)	7(7)	19(25)	0(0)	0(0)	49(23)	14(14)	2(6)	5.9
	10	5(13)	6(12)	8(7)	20(25)	1(1)	1(0)	41(22)	15(14)	3(6)	4.9
	30	6(15)	7(12)	8(6)	21(26)	2(2)	1(0)	38(20)	15(13)	3(6)	4.9
	70	7(26)	8(17)	8(3)	22(21)	3(7)	1(0)	33(9)	15(9)	4(8)	8.0
5	10	11(11)	10(11)	7(8)	24(24)	1(0)	1(0)	26(27)	14(14)	6(5)	0.8
	30	12(12)	10(12)	7(7)	24(23)	2(4)	1(0)	25(21)	14(14)	5(8)	1.6
	70	14(31)	11(17)	7(4)	24(19)	2(8)	1(0)	21(6)	14(6)	6(8)	6.9
6	10	34(15)	15(13)	4(7)	22(23)	1(3)	1(0)	8(19)	8(13)	8(7)	4.9
	30	35(20)	15(15)	4(6)	22(22)	2(5)	1(0)	7(13)	8(12)	8(7)	3.6
	70	36(44)	15(17)	4(3)	21(15)	2(7)	1(0)	6(3)	7(3)	8(9)	3.4
7	0	98(82)	1(7)	0(0)	1(8)	0(0)	0(0)	0(0)	0(0)	0(3)	3.7
	30	97(89)	1(5)	0(0)	1(4)	0(0)	0(0)	0(0)	0(0)	1(2)	1.8
	50	96(88)	2(6)	0(0)	2(5)	0(0)	0(0)	0(0)	0(0)	1(2)	1.9

^a In percentage points, calculated using pentad intensities including one value after the decimal point.

rotamers and rotational levels of the internal rotor become increasingly populated. An approximate treatment of these effects was thus performed for catalysts **4–6**.⁷⁰ The energy profile of 360° rotation of the alkyl was calculated for each of the four diastereomers, and all recorded minima and maxima (first-order saddle points) were included in the Boltzmann distribution.

Catalysts **4–6** (with a Me, Et and ^tPr substituent, respectively) are hemiisospecific, and low enantioselectivity for the (S) complexes have been reported in previous calculations.⁴³ As noted above for compound **3**, accurate estimates of the pentad distribution are hard to obtain for catalysts displaying low enantioselectivity (Table 2).

Whereas the calculated pentad distribution for the ethyl-substituted catalyst **5** is in excellent agreement with experiment at low temperatures (RMS deviation of <1 percentage point at 10 °C), the methyl and isopropyl-substituted catalysts are predicted to be too syndiospecific and too isospecific, respectively (Table 4). The latter deviations seem to be connected to the force field description of one particular angle.⁷⁰

Inclusion of effects due to rotation of the alkyl groups does result in an increase in predicted specificity with rising temperature, but the dramatic increase observed above 40–50 °C is by no means reproduced by the current approach. The substantial decrease in syndiospecificity for the related, unsubstituted compound (**1**) starts at equal temperatures, and we recall that back-skipping of the polymer chain is the most likely explanation for this decrease. For **1**, two consecutive insertions starting from the same monomer coordination site most probably will lead to an *m*-dyad (regarded as an error in syndiotactic polymer), and for the substituted catalysts **4–7**, this is true at least for one of the coordination sites [leading to an (R) diastereomeric monomer complex]. It is likely that the barrier to chain migration is lower when starting from the sterically less encumbered complexes (S) than from (R). Thus, for (S) diastereomers, chain migration will sooner be able to compete with insertion as temperature is rising, leading to an increasing fraction (>50%) of the insertions actually taking place for (R) diastereomers. And for (R) diastereomers, the propene *re*-face is preferred and the amount of isotactic polymer increases accordingly. In other words, back-skip (migration) of the

growing polymer chain seems to be the most likely explanation for the dramatic increase in specificity with temperature for catalysts **4–7** whereas temperature-induced rotation of the alkyl groups seems to be responsible for only a fraction of this increase. However, both the experimental and theoretical results suggest that back-skip is unimportant at low and ambient temperatures. For **7**, it has been claimed^{1,65} that insertion may proceed only from (R) complexes due to the large repulsive interaction between the polymer chain and the *tert*-butyl substituent resulting from insertion from the opposite monomer coordination site (S). However, hemiisotactic polypropene is obtained with **6**, confirming that insertion for “blocked” (S) complexes is possible despite the presence of a relatively large substituent (isopropyl). In addition, the calculated molecular mechanics energies for **7** (Table 2) indicate that the *Sre* TS is only 0.5 kcal/mol less stable than that of *Rre*.

Careful comparison of calculated and observed pentad distributions at a range of different temperatures thus indicates that back-skip is important for explaining the stereospecificity of **4–6** above 30–50 °C, but is unnecessary for explaining the observed isospecificity of **7**.

VII. Present State and Outlook

The clear relationship between the molecular structure of the catalyst and the resulting microstructure of the polymer was evident already in the earliest works in the field of modeling of stereospecificity of homogeneous propene polymerizing catalysts. In recent years, it has been possible and also meaningful through more realistic models of the intermediate and transition structures of the insertion process, to perform more detailed and quantitative comparison with experiment through calculation of the pentad distribution. It now seems as the structure of the catalyst cation is even more decisive than perhaps first imagined. Recent results indicate that, for polymerization with noncoordinating solvents at low and intermediate temperatures, pentad distributions can be predicted with semiquantitative accuracy at minimal cost and without inclusion of effects from solvent or counterion (cocatalyst).

The methods used so far in this field have largely been based on molecular mechanics, and it seems as remaining inaccuracies to some extent can be traced to specific problems in the force fields. Given the current development of computational schemes for treating large chemical systems (see, e.g., refs 97–102), there should be ample opportunity for improving the accuracy of the calculations compared to the current level. Hence, the nature of the relationship between catalyst structure and polymer tacticity will undoubtedly be further explored in the years to come. Increased accuracy will be of importance for mechanistic studies whereas low computational cost and ease of use probably will inspire more widespread application of these methods. The systematic investigation of the relationship between structural features of catalyst fragments and the microstructure of the resulting polymers should also allow for the creation of combinatorial libraries, see, e.g., ref 103, which can be used for a more rational, polymer-oriented development of catalysts for the stereospecific polymerization of α -olefins.

VIII. Acknowledgment

Recent research by the authors quoted or explicitly given herein was financially supported by the Research Council of Norway (Grant 119204/410). Access to supercomputer resources was granted by the Research Council of Norway (Program for Supercomputing), the Rechenzentrum der Gesellschaft für wissenschaftliche Datenverarbeitung in Göttingen, and the Rechenzentrum der MPG und IPP in Garching.

IX. References

- Brintzinger, H. H.; Fischer, D.; Mühlhaupt, R.; Rieger, B.; Waymouth, R. M. *Angew. Chem., Int. Ed. Engl.* **1995**, *34*, 1143.
- Jordan, R. F.; Dasher, W. E.; Echols, S. F. *J. Am. Chem. Soc.* **1986**, *108*, 1718.
- Allegra, G. *Makromol. Chem.* **1971**, *145*, 235.
- Cossée, P. *J. Catal.* **1964**, *3*, 80.
- Arlman, E. J. *J. Catal.* **1964**, *3*, 89.
- Arlman, E. J.; Cossée, P. *J. Catal.* **1964**, *3*, 99.
- Ewen, J. A. *J. Mol. Catal. A* **1998**, *128*, 103.
- Rappé, A. K.; Skiff, W. M.; Casewit, C. J. *Chem. Rev.* **2000**, *100*, 1435.
- Corradini, P.; Guerra, G.; Vacatello, M.; Villani, V. *Gazz. Chim. Ital.* **1988**, *118*, 173.
- Corradini, P.; Barone, V.; Fusco, R.; Guerra, G. *Eur. Polym. J.* **1979**, *15*, 1133.
- Corradini, P.; Guerra, G.; Fusco, R.; Barone, V. *Eur. Polym. J.* **1980**, *16*, 835.
- Corradini, P.; Barone, V.; Guerra, G. *Macromolecules* **1982**, *15*, 1242.
- Corradini, P.; Barone, V.; Fusco, R.; Guerra, G. *J. Catal.* **1982**, *77*, 32.
- Corradini, P.; Barone, V.; Fusco, R.; Guerra, G. *Gazz. Chim. Ital.* **1983**, *113*, 601.
- Corradini, P.; Busico, V.; Guerra, G. In *Transition Metals and Organometallics as Catalysts for Olefin Polymerization*; Kaminsky, W., Sinn, H., Eds.; Springer-Verlag: Berlin, Heidelberg, 1988.
- Cohen, S. A.; Auburn, P. R.; Bercaw, J. E. *J. Am. Chem. Soc.* **1983**, *105*, 1136.
- Cossée, P. In *The stereochemistry of macromolecules*; Ketley, A. D., Ed.; Marcel Dekker: New York, NY, 1967; Vol. 1.
- Hine, J. *J. Org. Chem.* **1966**, *31*, 1236.
- Hine, J. *Adv. Phys. Org. Chem.* **1977**, *15*, 1.
- Cahn, R. S.; Ingold, C.; Prelog, V. *Angew. Chem., Int. Ed. Engl.* **1966**, *5*, 385.
- Schlögl, K. *Top. Stereochem.* **1966**, *1*, 39.
- Hanson, K. R. *J. Am. Chem. Soc.* **1966**, *88*, 2731.
- Cavallo, L.; Guerra, G.; Oliva, L.; Vacatello, M.; Corradini, P. *Polym. Commun.* **1989**, *30*, 16.
- Venditto, V.; Guerra, G.; Corradini, P.; Fusco, R. *Polymer* **1990**, *31*, 530.
- Cavallo, L.; Guerra, G.; Vacatello, M.; Corradini, P. *Macromolecules* **1991**, *24*, 1784.
- Corradini, P.; Guerra, G. *Prog. Polym. Sci.* **1991**, *16*, 239.
- Cavallo, L.; Corradini, P.; Guerra, G.; Vacatello, M. *Polymer* **1991**, *32*, 1329.
- Cavallo, L.; Guerra, G.; Vacatello, M.; Corradini, P. *Chirality* **1991**, *3*, 299.
- Corradini, P.; Busico, V.; Cavallo, L.; Guerra, G.; Vacatello, M.; Venditto, V. *J. Mol. Catal.* **1992**, *74*, 433.
- Guerra, G.; Cavallo, L.; Venditto, V.; Vacatello, M.; Corradini, P. *Makromol. Chem., Macromol. Symp.* **1993**, *69*, 237.
- Corradini, P. *Makromol. Chem., Macromol. Symp.* **1993**, *66*, 11.
- Cavallo, L.; Guerra, G.; Corradini, P.; Resconi, L.; Waymouth, R. M. *Macromolecules* **1993**, *26*, 260.
- Guerra, G.; Cavallo, L.; Moscardi, G.; Vacatello, M.; Corradini, P. *J. Am. Chem. Soc.* **1994**, *116*, 2988.
- Guerra, G.; Corradini, P.; Cavallo, L.; Vacatello, M. *Macromol. Symp.* **1995**, *89*, 307.
- Corradini, P.; Guerra, G.; Cavallo, L.; Moscardi, G.; Vacatello, M. In *Ziegler Catalysts*; Fink, G., Mühlhaupt, R., Brintzinger, H. H., Eds.; Springer-Verlag: Berlin, 1995.
- Cavallo, L.; Guerra, G.; Corradini, P. *Gazz. Chim. Ital.* **1996**, *126*, 463.
- Cavallo, L.; Corradini, P.; Guerra, G.; Resconi, L. *Organometallics* **1996**, *15*, 2254.
- Guerra, G.; Cavallo, L.; Moscardi, G.; Vacatello, M.; Corradini, P. *Macromolecules* **1996**, *29*, 4834.
- Guerra, G.; Longo, P.; Cavallo, L.; Corradini, P.; Resconi, L. *J. Am. Chem. Soc.* **1997**, *119*, 4394.
- Guerra, G.; Cavallo, L.; Corradini, P.; Fusco, R. *Macromolecules* **1997**, *30*, 677.
- Toto, M.; Cavallo, L.; Corradini, P.; Moscardi, G.; Resconi, L.; Guerra, G. *Macromolecules* **1998**, *31*, 3431.
- Angermund, K.; Hanuschik, A.; Nolte, M. In *Ziegler Catalysts*; Fink, G., Mühlhaupt, R., Brintzinger, H. H., Eds.; Springer-Verlag: Berlin, Germany, 1995.
- van der Leek, Y.; Angermund, K.; Reffke, M.; Kleinschmidt, R.; Goretzki, R.; Fink, G. *Chem. Eur. J.* **1997**, *3*, 585.
- Clark, M.; Cramer, R. D., III; Van Opdenbosch, N. *J. Comput. Chem.* **1989**, *10*, 982.
- Dewar, M. J. S. *Bull. Soc. Chim. Fr.* **1951**, *18*, C71.
- Chatt, J.; Duncanson, L. A. *J. Chem. Soc.* **1953**, 2939.
- Wu, Z.; Jordan, R. F.; Petersen, J. L. *J. Am. Chem. Soc.* **1995**, *117*, 5867.
- Casey, C. P.; Hallenbeck, S. L.; Pollock, D. W.; Landis, C. R. *J. Am. Chem. Soc.* **1995**, *117*, 9770.
- Galakhov, M. V.; Heinz, G.; Royo, P. *Chem. Commun.* **1998**, 17.
- Woo, T. K.; Fan, L.; Ziegler, T. *Organometallics* **1994**, *13*, 432.
- Woo, T. K.; Fan, L.; Ziegler, T. *Organometallics* **1994**, *13*, 2252.
- Lohrenz, J. C. W.; Woo, T. K.; Ziegler, T. *J. Am. Chem. Soc.* **1995**, *117*, 12793.
- Yoshida, T.; Koga, N.; Morokuma, K. *Organometallics* **1995**, *14*, 746.
- Jensen, V. R.; Børve, K. J.; Ystenes, M. *J. Am. Chem. Soc.* **1995**, *117*, 4109.
- Woo, T. K.; Margl, P.; Ziegler, T. *Organometallics* **1997**, *16*, 3454.
- Jensen, V. R.; Børve, K. J. *Organometallics* **1997**, *16*, 2514.
- Krauledat, H.; Brintzinger, H. H. *Angew. Chem., Int. Ed. Engl.* **1990**, *29*, 1412.
- Castonguay, L. A.; Rappé, A. K. *J. Am. Chem. Soc.* **1992**, *114*, 5832.
- Hart, J. R.; Rappé, A. K. *J. Am. Chem. Soc.* **1993**, *115*, 6159.
- Pietsch, M. A.; K., R. A. *Polym. Mater. Sci. Eng.* **1996**, *74*, 420.
- Wiser, D. C.; Rappé, A. K. *Polym. Mater. Sci. Eng.* **1996**, *74*, 423.
- Mayo, S. L.; Olafson, B. D.; Goddard, W. A. *J. Phys. Chem.* **1990**, *94*, 8897.
- Kawamura-Kuribayashi, H.; Koga, N.; Morokuma, K. *J. Am. Chem. Soc.* **1992**, *114*, 2359.
- Kawamura-Kuribayashi, H.; Koga, N.; Morokuma, K. *J. Am. Chem. Soc.* **1992**, *114*, 8687.
- Yoshida, T.; Koga, N.; Morokuma, K. *Organometallics* **1996**, *15*, 766.
- Burkert, U.; Allinger, N. L. *Molecular Mechanics*; American Chemical Society: Washington, DC, 1982.
- Allinger, N. L. *J. Am. Chem. Soc.* **1977**, *99*, 8127.
- Yu, Z. T.; Chien, J. C. W. *J. Polym. Sci., Part A: Polym. Chem.* **1995**, *33*, 125.
- Yu, Z. T.; Chien, J. C. W. *J. Polym. Sci., Part A: Polym. Chem.* **1995**, *33*, 1085.
- Angermund, K.; Fink, G.; Jensen, V. R.; Kleinschmidt, R. *Macromol. Rapid Commun.* **2000**, *21*, 91.
- Vosko, S. H.; Wilk, L.; Nusair, M. *Can. J. Phys.* **1980**, *58*, 1200.
- Becke, A. D. *Phys. Rev. A* **1988**, *38*, 3098.
- Perdew, J. P.; Wang, Y. *Phys. Rev. B* **1992**, *45*, 13244.

- (74) Vernoijs, P.; Snijders, J. G.; Baerends, E. J. *Slater-type Basis Functions for the Whole Periodic System*; Department of Theoretical Chemistry, Free University: Amsterdam, The Netherlands, 1981.
- (75) Snijders, J. G.; Baerends, E. J.; Vernoijs, P. *At. Nucl. Data Tables* **1982**, *26*, 483.
- (76) ADF 2.3.0; Department of Theoretical Chemistry, Free University: Amsterdam, The Netherlands.
- (77) Baerends, E. J.; Ellis, D. E.; Ros, P. *Chem. Phys.* **1973**, *2*, 41.
- (78) te Velde, G.; Baerends, E. J. *J. Comput. Phys.* **1992**, *99*, 84.
- (79) Bovey, F. A. *High-Resolution NMR of Macromolecules*; Academic Press: New York, NY, 1972.
- (80) Zambelli, A.; Locatelli, P.; Bajo, G.; Bovey, F. A. *Macromolecules* **1975**, *8*, 687.
- (81) Randall, J. C. *Polymer Sequence Determination by the Carbon 13 NMR Method*; Academic Press: New York, NY, 1977.
- (82) Bovey, F. A. *Chain Structure and Conformation of Macromolecules*; Academic Press: New York, NY, 1982.
- (83) McQuarrie, D. A. *Statistical Thermodynamics*; Harper & Row: New York, NY, 1973.
- (84) SYBYL 6.5; Tripos Assoc. Inc., St. Louis, USA.
- (85) Resconi, L.; Piemontesi, F.; Camurati, I.; Sudmeijer, O.; Nifant'ev, I. E.; Ivchenko, P. V.; Kuz'mina, L. G. *J. Am. Chem. Soc.* **1998**, *120*, 2308.
- (86) Ewen, J. A.; Elder, M. J.; Jones, R. L.; Haspeslagh, L.; Atwood, J. L.; Bott, S. G.; Robinson, K. *Makromol. Chem., Macromol. Symp.* **1991**, *48/49*, 253.
- (87) Herfert, N.; Fink, G. *Makromol. Chem.* **1992**, *193*, 1359.
- (88) Bierwagen, E. P.; Bercaw, J. E.; W. A. Goddard, I. *J. Am. Chem. Soc.* **1994**, *116*, 1481.
- (89) Busico, V.; Cipullo, R. *J. Am. Chem. Soc.* **1994**, *116*, 9329.
- (90) Resconi, L.; Fait, A.; Piemontesi, F.; Colonna, M.; Rychlicki, H.; Zeigler, R. *Macromolecules* **1995**, *28*, 6667.
- (91) Busico, V.; Cipullo, R. *Makromol. Chem., Macromol. Symp.* **1995**, *89*, 277.
- (92) Busico, V.; Cipullo, R. *J. Organomet. Chem.* **1995**, *497*, 113.
- (93) Busico, V.; Cipullo, R. *J. Organomet. Chem.* **1998**, *558*, 219.
- (94) Leclerc, M. K.; Brintzinger, H. H. *J. Am. Chem. Soc.* **1995**, *117*, 1651.
- (95) Leclerc, M. K.; Brintzinger, H. H. *J. Am. Chem. Soc.* **1996**, *118*, 9024.
- (96) Miyake, S.; Okumura, Y.; Inazawa, S. *Macromolecules* **1995**, *28*, 3074.
- (97) Maseras, F.; Morokuma, K. *J. Comput. Chem.* **1995**, *16*, 1170.
- (98) Humbel, S.; Sieber, S.; Morokuma, K. *J. Chem. Phys.* **1996**, *105*, 1959.
- (99) Froese, R. D. J.; Humbel, S.; Matsubara, T.; Sieber, S.; Svensson, M.; Morokuma, K. *J. Phys. Chem.* **1996**, *100*, 19375.
- (100) Thiel, W. *Theochem-J. Mol. Struct.* **1997**, *398*, 1.
- (101) Mordasini, T. Z.; Thiel, W. *Chimia* **1998**, *52*, 228.
- (102) Woo, T. K.; Cavallo, L.; Ziegler, T. *Theor. Chem. Acc.* **1998**, *100*, 307.
- (103) Balkenhohl, F.; von dem Bussche-Hünnefeld, C.; Lansky, A.; Zechel, C. *Angew. Chem., Int. Ed. Engl.* **1996**, *35*, 2289.
- (104) The original artwork was slightly modified to improve clarity.

CR990373M